Quantitative evaluation of the low Earth orbit satellite based slant total electron content determination

Xinan Yue,[1] William S. Schreiner,[1] Douglas C. Hunt,[1] Christian Rocken,[1] and Ying-Hwa Kuo[1]

Received 1 April 2011; revised 24 May 2011; accepted 9 June 2011; published 29 September 2011.

[1] With the increased number of low Earth orbit (LEO) satellites equipped with GPS receivers, LEO based GPS observations play a more important role in space weather research because of better global coverage and higher vertical resolution. GPS slant total electron content (TEC) is one of the most important space weather products. In this paper, the LEO based slant TEC derivation method and the main error sources, including the multipath calibration, the leveling of phase to the pseudorange TEC, and the differential code bias (DCB) estimation, are described systematically. It is found that the DCB estimation method based on the spherical symmetry ionosphere assumption can obtain reasonable results by analyzing data from multiple LEO missions. The accuracy of the slant TEC might be enhanced if the temperature dependency of DCB estimation is considered. The calculated slant TEC is validated through comparison with empirical models and analyzing the TEC difference of COSMIC colocated clustered observations during the initial stage. Quantitatively, the accuracy of the LEO slant TEC can be estimated at 1–3 tecu, depending on the mission. Possible use of the LEO GPS data in ionosphere and plasmasphere is discussed.

Citation: Yue, X., W. S. Schreiner, D. C. Hunt, C. Rocken, and Y.-H. Kuo (2011), Quantitative evaluation of the low Earth orbit satellite based slant total electron content determination, *Space Weather*, *9*, S09001, doi:10.1029/2011SW000687.

1. Introduction

[2] Since the accomplishment of the global position system (GPS), the ground based total electron content (TEC) observations have dramatically enhanced our understanding on the ionosphere and many scientific researches using GPS TEC data have been published [*Mannucci et al.*, 1998]. In the past decade, many low Earth orbit (LEO) satellites were equipped with GPS receivers for either precise orbit determination (POD) or radio occultation (RO) observation (e.g., GPS/MET, CHAMP, GRACE, COSMIC, Jason, SAC-C, TerraSAR-X, Metop-A, C/NOFS, etc). The number of LEO based GPS observations would be significantly increased in the near future because many planned missions will be launched with the GPS payload [*Anthes*, 2011].

[3] Through decoding the received GPS signals, the carrier phase and pseudorange of both GPS frequencies can be derived. These observations can then be applied to calculate the TEC data contributed by both the ionosphere and the plasmasphere along the GPS ray. These TEC data have shown valuable applications in both scientific research of ionosphere and plasmasphere and in space weather monitoring [*Bust et al.*, 2007; *Coster and Komjathy*, 2008; *Hajj et al.*, 2000; *Heise et al.*, 2002; *Jakowski et al.*, 2007; *Mannucci et al.*, 2005; *Pedatella and Larson*, 2010]. In higher altitude orbit like COSMIC satellites (~800 km), high elevation observations can usually be used to study the plasmasphere, e.g., *Pedatella and Larson* [2010] applied COSMIC slant TEC data to determine the position of the plasmapause; both *Heise et al.* [2002] and *Jakowski et al.* [2007] tried to image the 3-D topside ionosphere and plasmasphere by assimilating the CHAMP TEC data into the model. For ionospheric storm study, LEO slant TEC data allow the researchers to distinguish the storm response of ionosphere and plasmasphere as has been done by *Mannucci et al.* [2005] and *Pedatella et al.* [2009]. As we know, both the LEO and GPS satellites are moving with a high speed in the space. Furthermore, the LEO GPS TEC has a much higher vertical resolution because it can have low or negative elevation observations. These factors make LEO GPS TEC being an ideal data source of iono-

[1]COSMIC Program Office, University Corporation for Atmospheric Research, Boulder, Colorado, USA.

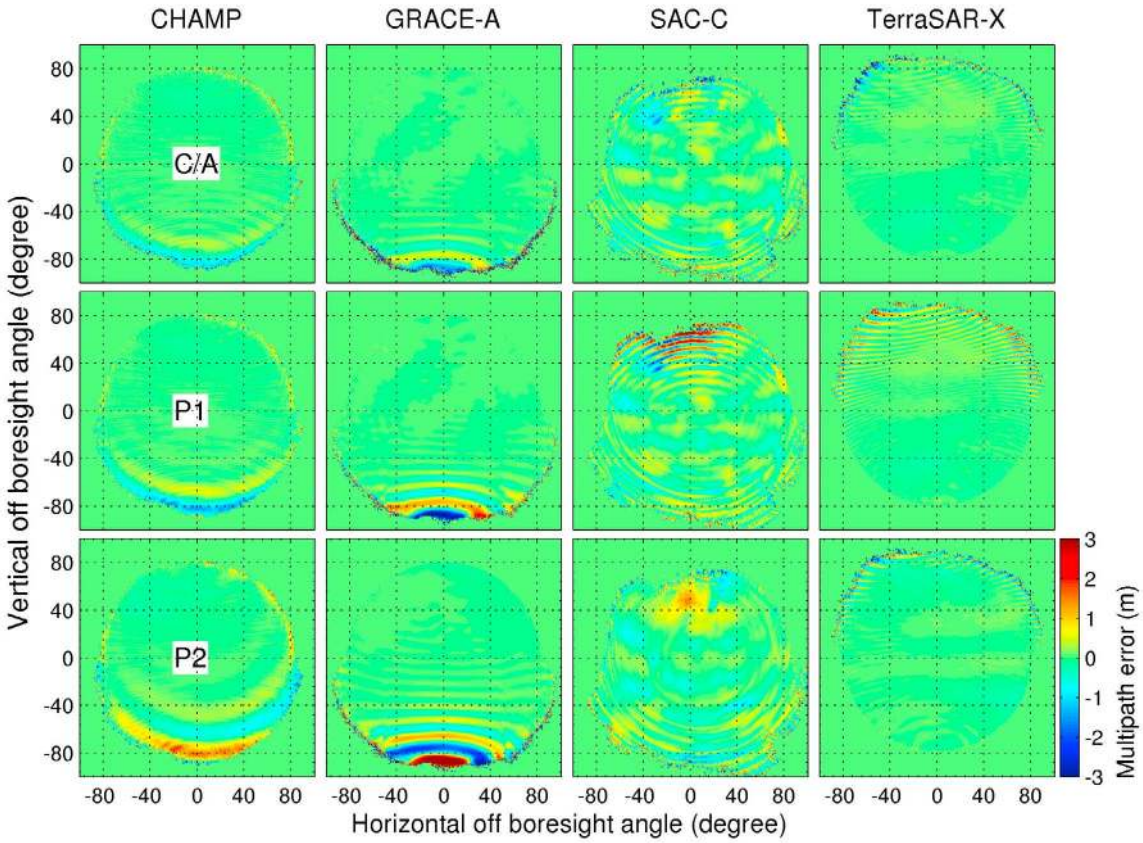

Figure 1. Estimated multipath errors (meter) of pseudorange of (top) C/A, (middle) P1, and (bottom) P2 code for the POD antenna on board CHAMP, GRACE, SAC-C, and TerraSAR-X satellites versus the vertical and horizontal components of the off boresight angle.

spheric data assimilation [*Komjathy et al.*, 2010; *Pi et al.*, 2009; *Scherliess et al.*, 2009; *Yue et al.*, 2011]. Through assimilating the COSMIC slant TEC into JPL/USC-GAIM, *Komjathy et al.* [2010] found better improvements in NmF2, hmF2, and vertical TEC specifications than only using ground based observations. *Pi et al.* [2009] assimilated the COSMIC TEC data into the model and successfully tracked the 3-D structure of ionosphere during disturbed conditions. The ionospheric drivers such as wind and electric field can be estimated by assimilating a variety of data into the model as did by *Scherliess et al.* [2009]. This is of great significance for ionospheric short-term forecasting. In addition, some TEC observations with negative elevations can be used to derive an electron density profile (EDP) along the tangent points, which is called occultation observation [*Schreiner et al.*, 1999; *Yue et al.*, 2010].

[4] In comparison with ground based GPS observations, LEO GPS observations have the advantages of high vertical resolution and global distribution. Up-to-date, the calculation of TEC from ground based GPS, including combining the phase and pseudo range observations, cycle-slip detection, multipath elimination, and differential code bias (DCB) estimation, has been relatively mature [*Blewitt*, 1990; *Sardón et al.*, 1994]. However, when applying these procedures to the LEO based GPS observations, we would be confronted with some issues given below because of the quick movement and occasionally sharply varied attitude of the LEO satellite. Multipath is one kind of receiver error caused by the superposition of the direct signal with interfering signals taking a different propagation path [*Montenbruck and Kroes*, 2003]. For ground based GPS, the multipath effect can usually be minimized by discarding low elevation observations and specific antenna design. While for LEO GPS, the multipath effect is worse-than-expected due to the solar panels and usually used patch antennas [*Hwang et al.*, 2010]. When estimating the receiver bias for LEO GPS, the usually used method for the ground based GPS is not applicable anymore because of the quick movement of the receiver [*Sardón et al.*, 1994]. For some LEO satellites, the sur-

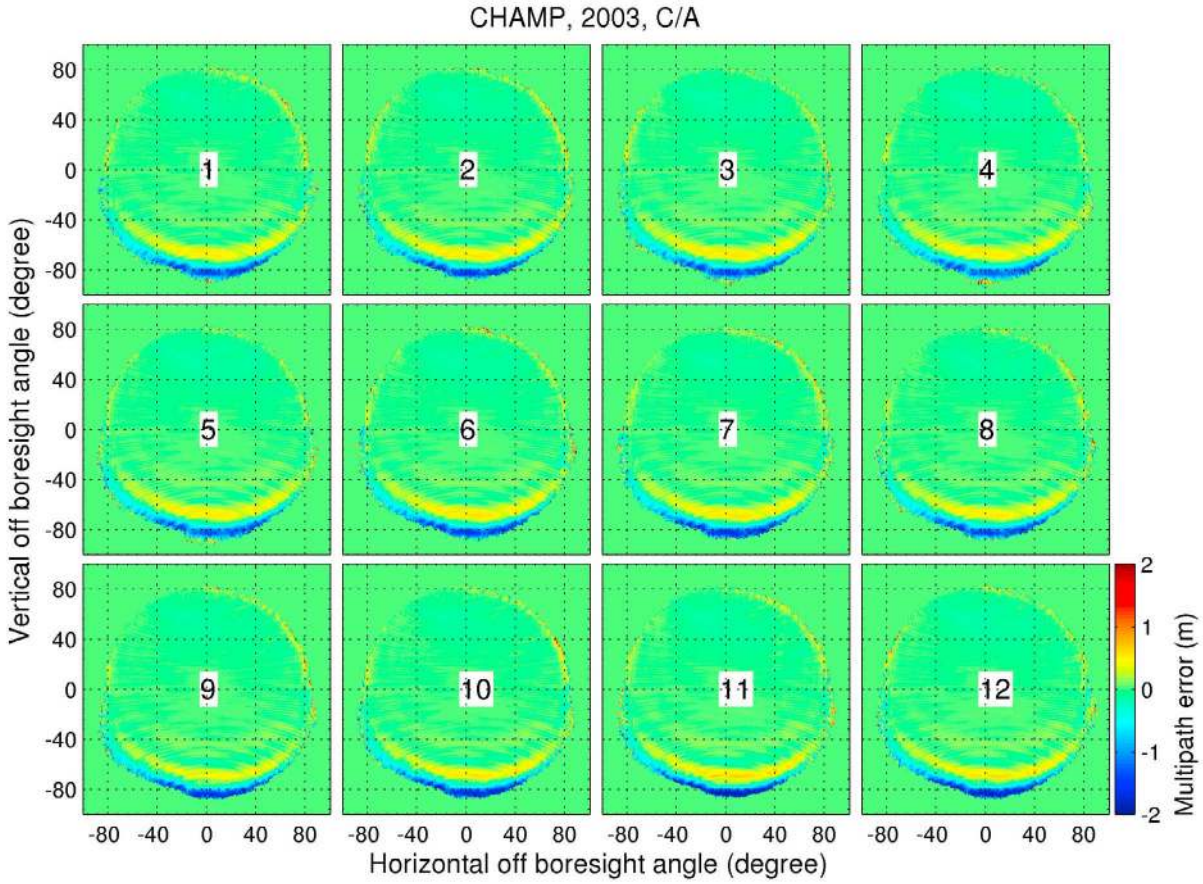

Figure 2. Multipath errors (meter) of C/A pseudorange of CHAMP POD antenna during separate months of 2003. The number in the subplot is the corresponding month.

rounding temperatures change sharply from orbit to orbit. This might challenge the generally used assumption of the constant DCB during a certain time on the DCB estimation. In addition, the high elevation LEO based TEC value is usually very small (1–2 tecu, 1 tecu = 10^{16}m^{-2}) in the nighttime and is so comparable with the TEC accuracy especially for some high altitude orbit satellites. It requires a much higher accuracy of LEO based TEC to make it more useful.

[5] With the increased number of the planned LEO missions equipped with the GPS receivers in the near future, LEO based GPS observations will play a more important role in the space weather field. However, the data property and quality of LEO GPS observations especially TEC data is still not recognized by some people. In this paper, we will give a systematical description on the data and the data quality of LEO based slant TEC especially from the prospect of space weather. We will mainly focus on the current data processing in the COSMIC data analysis and archive center (CDAAC) of the university corporation for atmospheric research (UCAR). The calculation of slant TEC from LEO GPS is given in section 2. In section 3 we will show some evaluation results. We then discuss and conclude in sections 4 and 5, respectively.

2. LEO TEC Calculation

[6] The GPS observation functions of the pseudorange and carrier phase, which will be used to calculate TEC, can be generally expressed as follows [*Hajj et al.*, 2000; *Sardón et al.*, 1994]:

$$P_k^{ij} = p_{ij} + p^{trop} + p_k^{iono} + b_k^i + b_k^j + MP_{P_k} + \sigma_{p_k} \quad (1)$$

$$L_k^{ij} = n_k^{ij}\lambda_k + l_{ij} + l^{trop} + l_k^{iono} + b_k^i + b_k^j + MP_{l_k} + \sigma_{l_k} \quad (2)$$

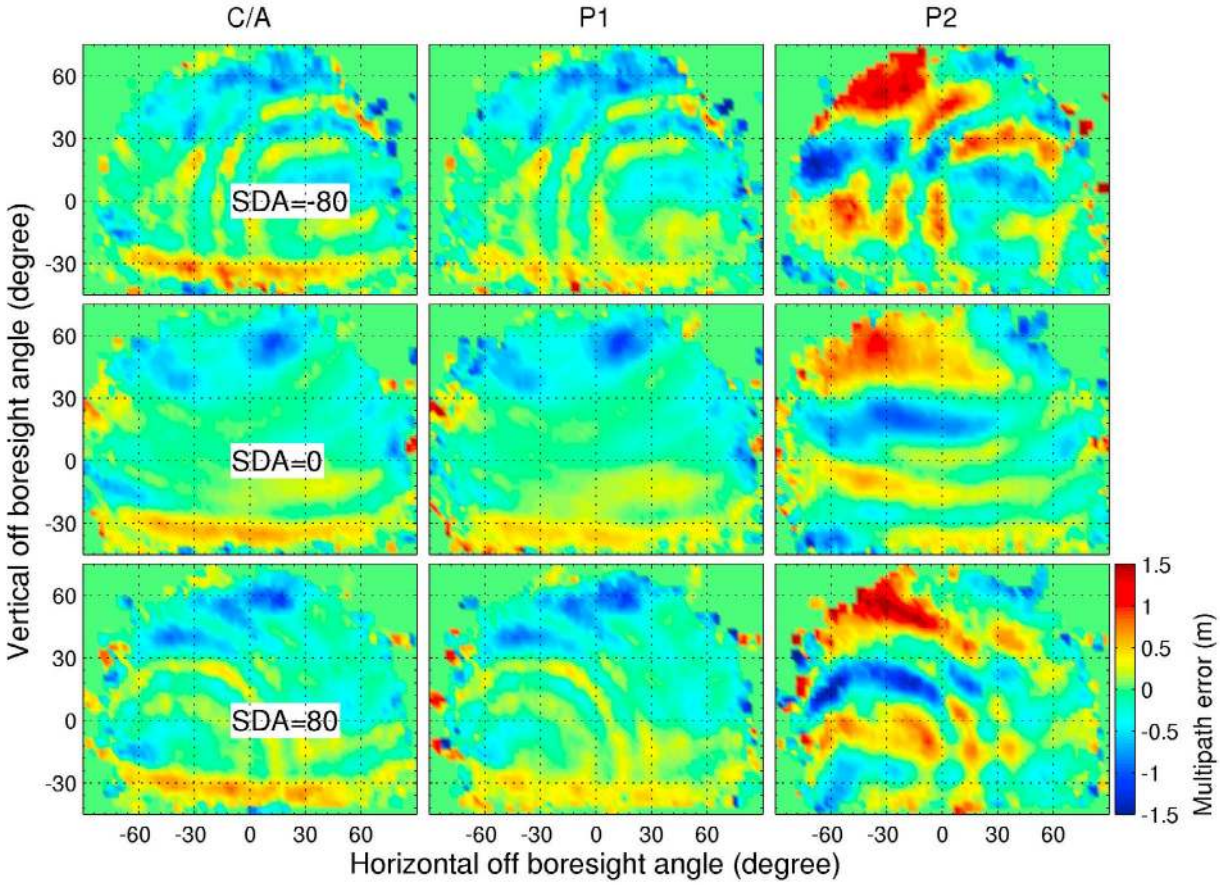

Figure 3. Multipath errors (meter) of (left) C/A, (middle) P1, and (right) P2 pseudorange of COSMIC FM4 antenna 1 (POD) when solar array drive angle is (top) –80, (middle) 0, and (bottom) 80 degree.

where i and j represents the transmitter and receiver, respectively; k is for f1 (1.57542×10^9 Hz) or f2 (1.2276×10^9 Hz) frequencies; P and L are the corresponding observed pseudorange and carrier phase, respectively; The first item of the right hand side of function (2) is called integer ambiguity; p_{ij} (l_{ij}), p^{trop} (l^{trop}), and p^{iono} (l^{iono}) are the real range (phase) with vacuum assumption between the transmitter and receiver, tropospheric delay, and frequency dependent ionospheric delay, respectively; b, MP, and σ represents the bias, multipath, and observation error, respectively.

[7] Before processing the data, the outliers and cycle slip are eliminated by the approach suggested by *Blewitt* [1990] in CDAAC. As pointed out by *Hwang et al.* [2010], the LEO GPS observations suffer more frequent occurrence of cycle slip and outliers because of the quick movement of the receiver and relatively low signal-to-noise ratio (SNR) especially under low elevation observations [*Montenbruck and Kroes*, 2003]. After removing the outliers and cycle slip of the carrier phase on L1 and L2, the following combination is used to estimate the bias for pseudorange observations:

$$d_k = P_k + \left\{ \begin{array}{l} \left(2 \times L_2 \times f_2^2 - L_1 \times \left(f_1^2 + f_2^2\right)\right)/\left(f_1^2 - f_2^2\right), k = 1 \\ \left(-2 \times L_1 \times f_1^2 + L_2 \times \left(f_1^2 + f_2^2\right)\right)/\left(f_1^2 - f_2^2\right), k = 2 \end{array} \right\} \tag{3}$$

$$\sigma_k = \frac{d_k^i \times SNR_k^{i^2}}{\sum_i SNR_k^{i^2}} \tag{4}$$

where k represents the pseudorange of f1 (P1,C1) or f2 (P2); L1 and L2 is phase observation; f1 and f2 are two

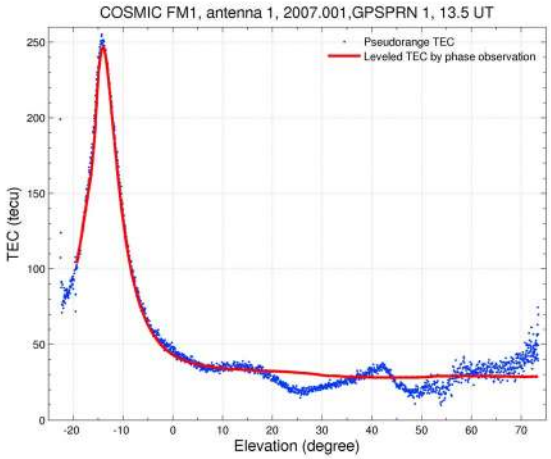

Figure 4. An example shows the original pseudorange TEC (dot) and the leveled TEC (line) by the phase observations after multipath calibration observed by the COSMIC FM1 satellite during 2007.001.

frequencies; σ_k represents the corresponding bias of the pseudorange, which was obtained by weighting with the inverse of the square of the SNR. Then, the multipath errors of the pseudorange observations can generally be estimated by the following so-called multipath combinations:

$$M_k = d_k - \sigma_k \tag{5}$$

[8] For a specific GPS antenna, the corresponding multipath errors of C/A and P code (P1 and P2) can be calculated by using pseudorange and phase observations during a certain time. As an example, Figure 1 shows the estimated multipath errors of C/A, P1 and P2 pseudorange for the POD antenna on board CHAMP, GRACE, SAC-C, and TerraSAR-X satellites in CDAAC. As can be seen, the distribution of the multipath error depends on the configuration of the satellite and the antenna as stated by *Montenbruck and Kroes* [2003]. For CHAMP and GRACE-A POD antenna, the occurrence of the multipath error is close to the satellite horizon of the after looking hemisphere. This is probably due to the cross-talk between the POD and occultation antenna strings within the BlackJack receiver as demonstrated by *Montenbruck and Kroes* [2003]. In comparison with CHAMP and GRACE-A POD antenna, the multipath pattern of SAC-C and TerraSAR-X POD antenna is a little bit more complicated. It might be related to the more complicated configuration of the solar array panel and different antenna design. Furthermore, the amplitude and pattern of the multipath errors are not exactly the same among C/A, P1 and P2 because of the difference of the wavelength. Usually, the multipath pattern does not change with time for a specific antenna [*Montenbruck and Kroes*, 2003]. As an example, Figure 2 shows the CHAMP POD antenna C/A code multipath errors estimated for every separate months during 2003. No month to month variations of either the amplitude or the distribution pattern of the multipath error are detected. The multipath varies only with respect to the off boresight angles for CHAMP, GRACE, SAC-C, and TerraSAR-X satellites. But for some other satellites like COSMIC, the multipath also depends on the solar array drive angle (SDA). Figure 3 gives the multipath errors of COSMIC FM4 antenna 1 C/A, P1, and P2 pseudorange for SDA = −80, 0, and 80 degrees, respectively. As shown in the figure, the multipath has an obvious SDA dependency. Furthermore, the COSMIC multipath is smaller than that of CHAMP and GRACE because of its relatively smaller satellite size. After getting the multipath error distributions as displayed in Figures 1–3, the multipath can be calibrated by subtracting these errors from original observations. Please note that nonlocal multipath such as reflection from the ocean surface might not be eliminated effectively by this method.

[9] For dual frequency GPS receiver, absolute and relative slant TEC can be obtained by taking linear combination of the pseudorange and carrier phase, respectively [*Sardón et al.*, 1994]. A leveling algorithm to the absolute TEC of the relative TEC is normally used because relative TEC has much higher accuracy than that of the absolute TEC [*Mannucci et al.*, 1998]. Usually the leveling is implemented by weighting with the corresponding SNR, which is illustrated as follows:

$$TEC = \frac{f_1^2 \times f_2^2}{40.3 \times (f_1^2 - f_2^2)} \times (L_1 - L_2 + \sigma_{P_2} - \sigma_{P_1}) \tag{6}$$

where σ is the corresponding bias estimated by functions (3) and (4). The unit of L, σ, and TEC is, meter, meter, and tecu, respectively. Figure 4 shows a comparison example between the original pseudorange TEC and the leveled TEC by the phase observations after multipath calibration observed by the COSMIC FM1 satellite during 2007.001. Note that the DCB of GPS satellite and receiver is not calibrated here. For every GPS arc, the leveling error is estimated by the following formula:

$$\frac{\sqrt{\sum_{i=1}^{n} (TEC_L - TEC_p)^2}}{n} \tag{7}$$

where n is the observation number for the specific GPS arc; TEC_L and TEC_P is the leveled and pseudorange TEC, respectively. Figure 5 gives the leveling errors of the observations from COSMIC FM2 during 2006–2011. One dot represents one GPS arc. The daily average leveling error (circle) is also given. For both antennas, the leveling error varies between 0 and 0.7 tecu and the average value is

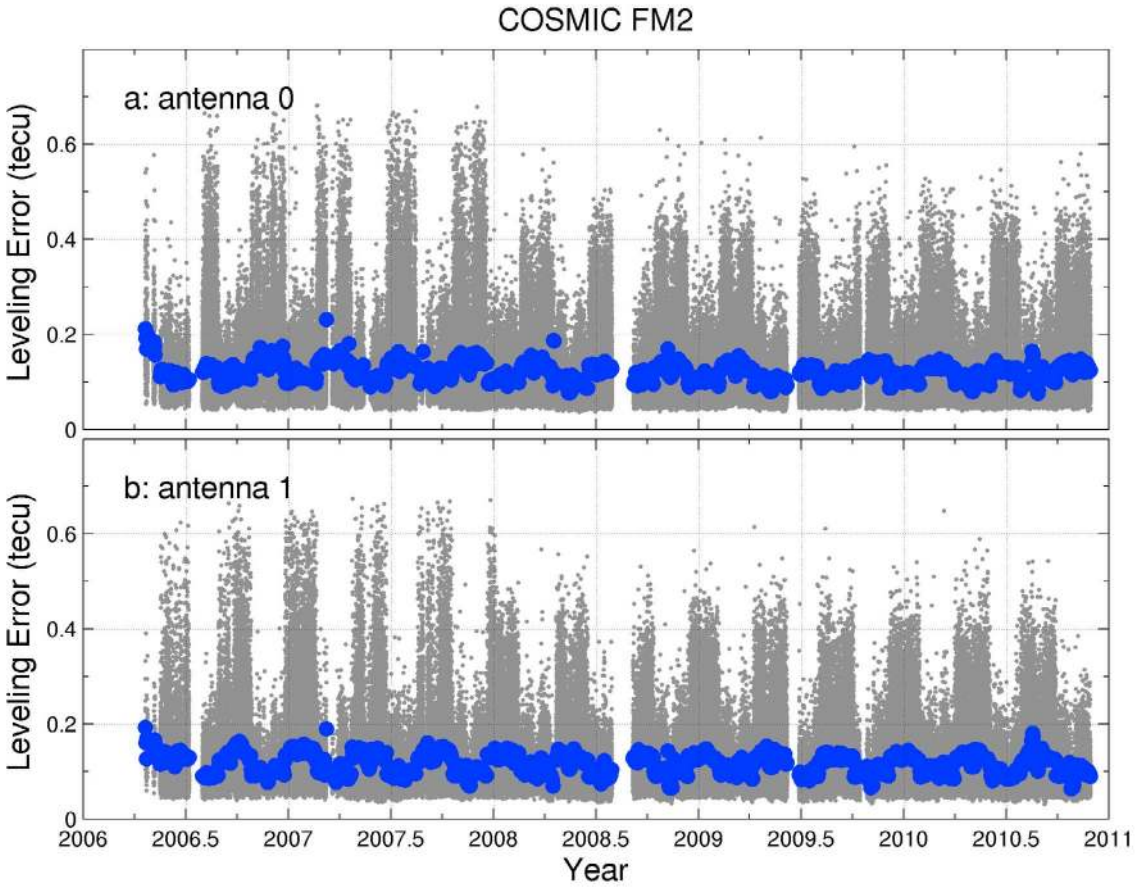

Figure 5. Leveling error of COSMIC FM2 antenna (a) 0 and (b) 1 during 2006–2011. One dot represents one GPS arc, while the circle is daily average.

~0.1 tecu. The discontinuity versus years is due to the receiver turn off or bad data quality.

[10] In CDAAC, the GPS satellite DCB is calibrated using the center for orbit determination in Europe (CODE) results, which were obtained by a least square fit method based on global ground based GPS observations [*Schaer*, 1999]. Many different methods have been proposed to estimate the ground based GPS receiver DCB [*Mannucci et al.*, 1998; *Sardón et al.*, 1994; *Schaer*, 1999]. Basically, it is a least square fit solution based on some different kinds of parameterization of local, regional, or global ionosphere. However, for the LEO based GPS receiver, it is not applicable to estimate the DCB by parameterization of the ionosphere because of the movement of the satellite. Usually, the LEO satellite is flying above the F layer of the ionosphere. The spherical symmetry assumption, which is used in the electron density profile retrieval from radio occultation measurements [*Yue et al.*, 2010], is generally applicable. Under this assumption, the simultaneous two observations (TEC_1 and TEC_2 with the DCB of GPS satellites calibrated) from two GPS satellites of one LEO antenna can be related by

$$(TEC_1 + DCB) \times m(\varepsilon_1) = (TEC_2 + DCB) \times m(\varepsilon_2) \tag{8}$$

$$m(\varepsilon) = \frac{\sin\varepsilon + \sqrt{(r_{ion}/r_{orb})^2 - (\cos\varepsilon)^2}}{1 + r_{ion}/r_{orb}} \tag{9}$$

where DCB is the GPS receiver antenna bias to be estimated; m is the geometric mapping function proposed by *Foelsche and Kirchengast* [2002]; ε, r_{ion}, and r_{orb} is the elevation angle of GPS ray, ionospheric and satellite altitude from the Earth center, respectively. r_{ion} can be selected to be several hundreds or thousands of kilometers above the satellite orbit altitude, and this parameter will not significantly influence the estimated DCB by our test. Usually the DCB of one specific antenna can be assumed to be stable during one day [*Mannucci et al.*, 1998; *Sardón et al.*, 1994; *Schaer*, 1999]. For most LEO GPS receivers, more than

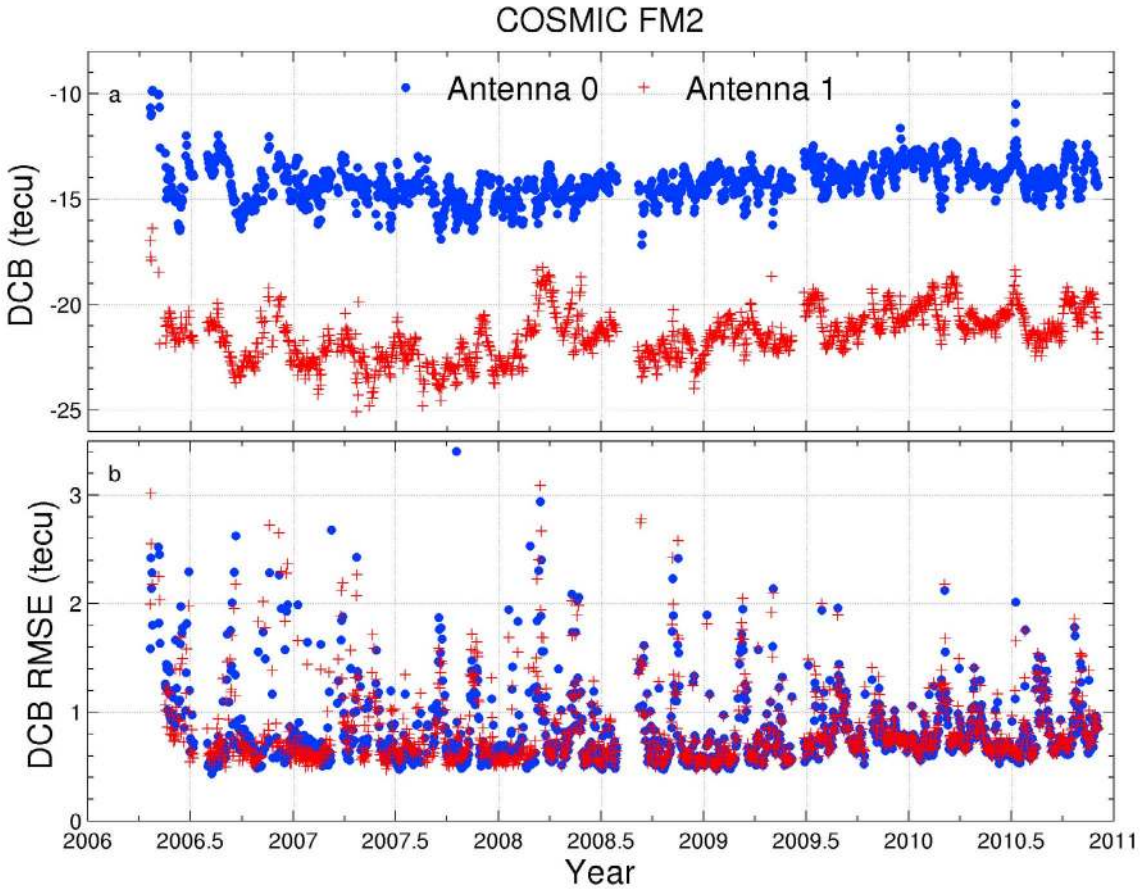

Figure 6. (a) DCB and (b) DCB RMSE of COSMIC FM2 satellite antenna 0 (circle) and 1 (cross) during 2006–2011.

10 GPS satellites can be tracked simultaneously. So there might be more than thousands of observation data pairs available during one day, which can be applied to estimate the DCB using functions (8)–(9). A least square solution is therefore derived through

$$\frac{-\sum_i \left[\left(m\left(\varepsilon_1^i\right) - m\left(\varepsilon_2^i\right)\right) \times \left(tec_1^i \times m\left(\varepsilon_1^i\right) - tec_2^i \times m\left(\varepsilon_2^i\right)\right)\right]}{\sum_i \left(m\left(\varepsilon_1^i\right) - m\left(\varepsilon_2^i\right)\right)^2} \quad (10)$$

[11] The root mean square error (RMSE) of the DCB is presented as

$$RMSE = \frac{\sqrt{\sum_i^n \left(DCB^i - \overline{DCB}\right)^2}}{n} \quad (11)$$

where DCB^i is the DCB estimated by the i^{th} observation pair using formula (8) and $\overline{DCB}$ is the least square solution

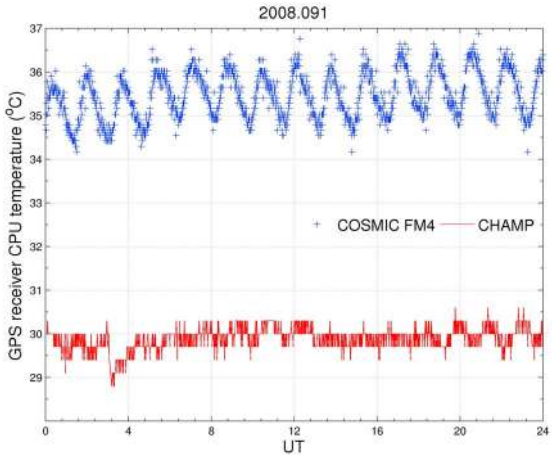

Figure 7. Daily GPS receiver CPU temperature of COSMIC FM4 (cross) and CHAMP (line) during 2008.091.

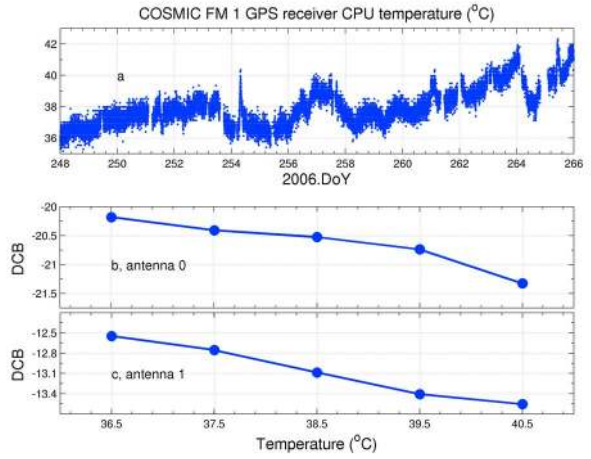

Figure 8. (a) COSMIC FM1 GPS receiver CPU temperature variations during 2006.248–265; (b) COSMIC FM1 antenna 0 DCB varies with respect to the receiver CPU temperature during 2006.248–265; (c) the same as Figure 8b, but for the antenna 1.

using all n data pairs. To decrease the RMSE of the DCB estimation, only the observations with higher elevation, from middle and high latitudes, and happening in the nighttime are selected to satisfy the spherical symmetry assumption at the best. The DCB and DCB RMSE of COSMIC FM2 antennas 0 and 1 during 2006–2011 are plotted in Figure 6 as an example. Generally, the variation of DCB of both antennas is within 5 tecu. But the DCB shows obvious day to day variability. The RMSE varies between 0 and 3 tecu and the average value is ~0.7 tecu. The other COSMIC satellites behave the same as FM2 (not shown here).

[12] In comparison with CHAMP (shown in Figure 9), the COSMIC DCB is much more noisy. This is probably due to the significant variations of the temperature of the receiver and the antenna of COSMIC during one day because the COSMIC receiver is directly shown up in the air [*Rideout and Coster*, 2006]. The big variation of the receiver temperature during one day will make the constant DCB assumption not applicable. In contrast, the CHAMP has a more stable daily temperature because the receiver is inside the satellite. Usually, the daily variability of COSMIC satellite receiver temperature can be bigger than 3°C, while it is less than 1°C for CHAMP. As an example, Figure 7 gives a comparison of the normal daily variation of the COSMIC FM4 and CHAMP GPS receiver CPU temperature during 2008.091. Please note that this is the normal operational situation. The receiver temperature can change very much when suffering rebooting or turning off. In addition, the COSMIC receiver CPU temperature is also an indication of the environment temperature, which has an influence up on the receiver antenna.

[13] To illustrate the possible effect of the temperature on the DCB value pointed out by *Rideout and Coster* [2006], we chose the continuous observations of COSMIC FM 1 during 2006.248–265 to do the test. The variations of the receiver CPU temperature during 2006.248–265 are plotted in Figure 8a. We assume the only factor that influences the DCB value is the temperature during this interval. The observations are then binned with respect to the temperature. The DCBs are estimated for different temperature interval. The test results are shown in Figures 8b and 8c. As illustrated in the figure, the DCB amplitude of both antennas linearly increases with the increase of the receiver CPU temperature.

[14] The DCB and DCB RMSE of CHAMP POD antenna are displayed in Figure 9. The DCB shows more smoothed day-to-day variation and smaller RMSE than that of COSMIC POD antenna. However, the CHAMP DCB also has some long-term drift and period variation. The F10.7 index and the orbit altitude are also given in the Figure 9. As can be seen, the long-term decrease of the DCB during 2002–2008 might be due to the decrease of the solar radiation represented by the F10.7 index. The short-term period is almost comparable with the period that the satellite covers all the local times. It implies that the period variations of the DCB might be related to the period variations of the received solar radiation and environment temperature on the satellite orbit due to the local time variation. As an illustration, the MSIS modeled daily CHAMP orbit neutral temperature is calculated during 2002–2008 and shown in the Figure 9. The model inputs include the F10.7 index, orbit altitude, latitude, longitude and local time. Daily neutral temperature is obtained by averaging the whole day data. It is found that the neutral temperature accords well with the DCB value in either long-term drift or period variations. This accordance confirms the effect of the environment radiation and temperature on the antenna DCB.

3. LEO TEC Evaluation

[15] To evaluate the quality of the LEO TEC data obtained by the above method, we first compare the calculated TEC data with the original pseudorange TEC. Both TECs are calibrated by the same DCBs. So this comparison will mainly include the errors of the leveling and multipath calibration. Figure 10 shows a comparison example of original pseudorange and CDAAC processed TEC data observed by COSMIC FM 1 antenna 1 during 2007.001 by tracking GPS PRN 4. From either the elevation or the universal time variation, the CDAAC processed TEC data can track the original pseudorange TEC well. But the processed TEC is smoother than the pseudorange TEC since the multipath has been calibrated and the pseudorange errors are eliminated by the leveling process. Figure 11 gives statistical results of the difference between CDAAC processed TEC and the original pseudorange TEC on COSMIC satellites observations over 10 days

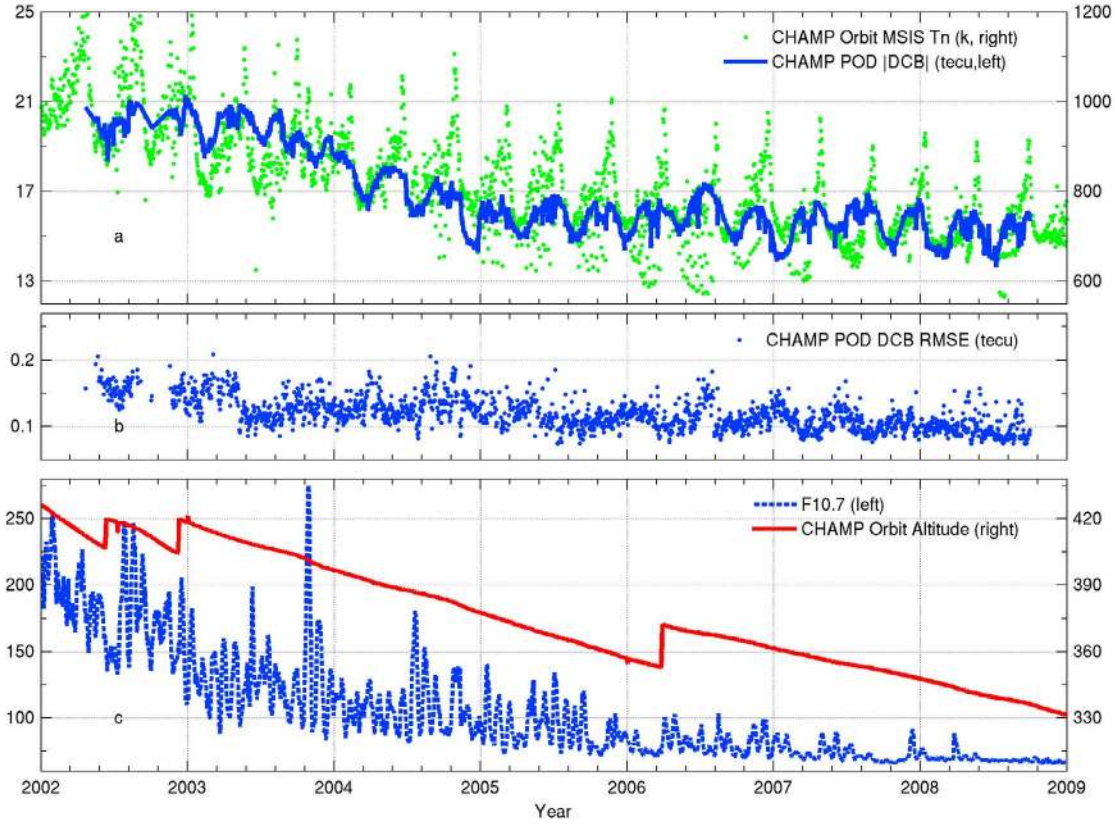

Figure 9. (a) Absolute value of CHAMP POD antenna DCB (line) and daily neutral temperature on CHAMP orbit (dot) during 2002–2008; (b) the corresponding DCB RMSE; (c) F10.7 index (dashed line) and CHAMP orbit altitude (km) during 2002–2008.

observations. The TEC difference shows a typical Gaussian distribution with the mean value is equal to –0.046 tecu. No local time or elevation dependences of the TEC difference is detected (not shown here). Statistically, the multipath errors and the pseudorange uncertainties can be assumed to be evenly distributed. So the statistical results in Figure 11 illustrate that our processed TEC has no systematic bias.

[16] *Schreiner et al.* [2007] used to estimate the precision of the COSMIC RO retrieved temperature and electron density profiles by comparing the colocated RO events when the satellites were clustered together in the initial stage. We borrow ideas from them here to evaluate the slant TEC data by comparing the colocated TEC observations. Figure 12 shows 3 occultation TEC observations from COSMIC satellites FM 1, 2, and 3 by tracking GPS PRN 24 within 1 min and the corresponding TEC difference. These colocated observations accord with each other very well. The difference between colocated pairs has a stable variation with the elevation. Since the colocated pairs track the same GPS satellite, the TEC difference mainly includes the errors of observation uncertainty, leveling process, multipath calibration, and the receiver DCB estimation. To make a statistical evaluation, we searched all this kind of colocated pairs with the difference of the tangent point latitude and longitude less than 2.5 degrees and time difference less than 1.2 min for all the COSMIC observations during 2006. There are totally 44464 pairs can be found and the statistical results are given in Figure 13. The absolute value of the average difference is 0.12 tecu and the RMSE of the difference is 1.36 tecu. If we analyze the TEC difference for different satellite antenna (e.g., FM 1 antenna 0 and FM 2 antenna 0) combinations, the absolute value of the average difference and the RMSE varies in the range of 0–0.7 tecu and 1.1–1.8 tecu, respectively. No obvious local time and elevation dependencies are detected. Please note that the

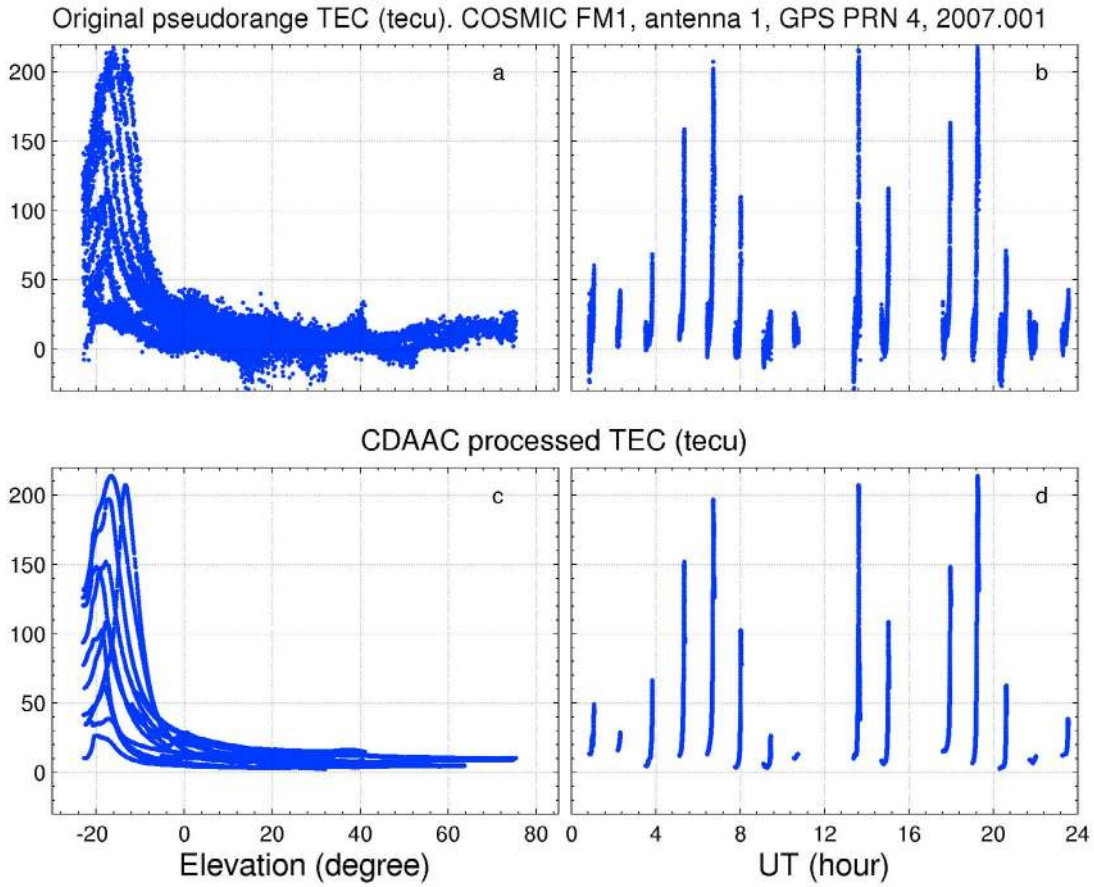

Figure 10. (a, b) Original pseudorange TEC and (c, d) the corresponding CDAAC processed TEC versus elevation (Figures 10a and 10c) and UT (Figures 10b and 10d) of COSMIC FM1 antenna 1 observations from GPS PRN 4 during 2007.001.

TEC difference might be influenced by the ionospheric local variability here.

[17] A common way to evaluate a type of observation is comparing with the model. Figure 14 shows a comparison example between COSMIC FM 1 observed and IRI2007 modeled slant TEC during an occultation event [*Bilitza*, 2009]. The plasmasphere is represented by the Gallagher plasmaspheric model [*Gallagher et al.*, 1988]. The observations and the modeling results agree generally well except overestimation of the model results during the low elevation observation. The accuracy of the slant TEC data will mainly influence the high elevation observations because of the relatively smaller amplitude of the plasmasphere TEC. To evaluate the slant TEC during high elevation, we select the COSMIC observed slant TEC with elevation bigger than 60° during 2008 spring. The slant TEC are then converted to the vertical TEC using a geometric mapping function [*Foelsche and Kirchengast*, 2002]. The pierce point is chosen to be 3000 km altitude. A vertical TEC map is created with respect to magnetic local

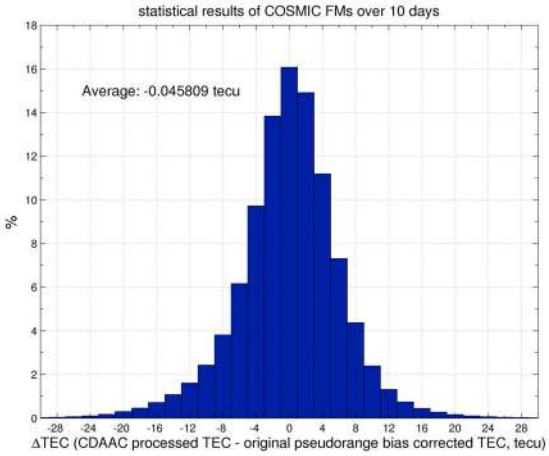

Figure 11. Statistical results of the difference between CDAAC processed TEC and the original pseudorange TEC of COSMIC satellites over 10 days.

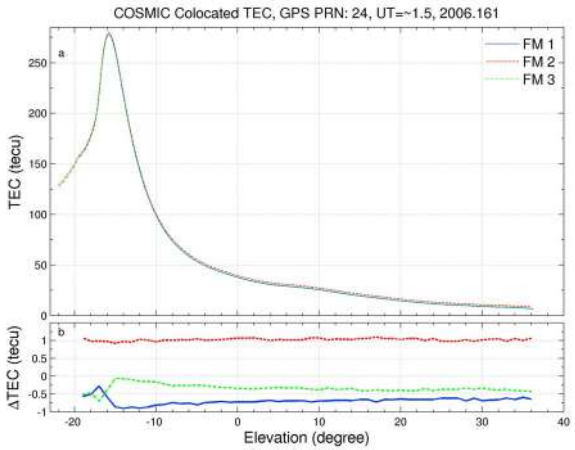

Figure 12. (a) An example of colocated TEC observations from COSMIC FM 1 (solid line), 2 (dashed line), and 3 (dash-dotted line) by tracking GPS PRN 24 simultaneously. (b) The TEC difference of colocated TEC from the averages of three satellites measurements.

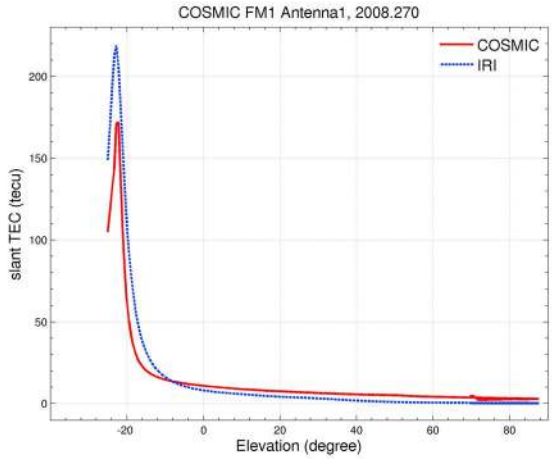

Figure 14. Comparison example between COSMIC FM1 observed and IRI2007 modeled slant TEC versus elevation during an occultation event.

time (MLT) and magnetic latitude (MLat) and compared with the model results as illustrated in Figure 15. The topside ionosphere and plasmasphere is represented by the IRI2007 model and the Gallagher plasmaspheric model, respectively [*Bilitza*, 2009; *Gallagher et al.*, 1988]. From either the amplitude or the MLT and MLat variations, the COSMIC observations accord well with the model results. It certifies the validity of the high elevation observations.

4. Discussion

[18] In the above sections, we gave a general description on the LEO satellite based slant TEC calculation. The main error sources including multipath calibration, phase leveling to the pseudorange, and DCB estimation are analyzed. Actually, some other factors might influence the slant TEC accuracy too. These factors include the GPS ray

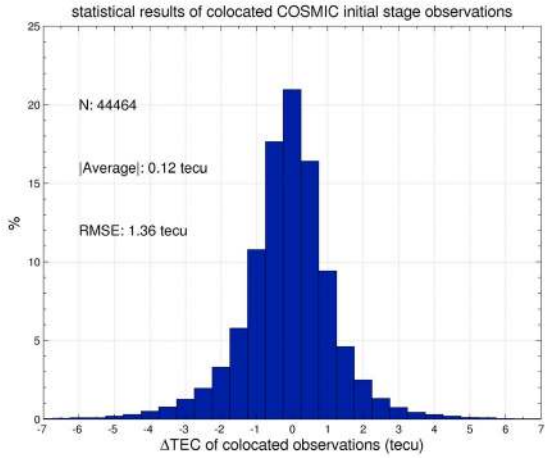

Figure 13. Statistical results of the difference between colocated TEC observation pairs during 2006.111–365 of COSMIC observations. The colocated pair number, absolute value of the average difference and RMSE of the difference are shown too.

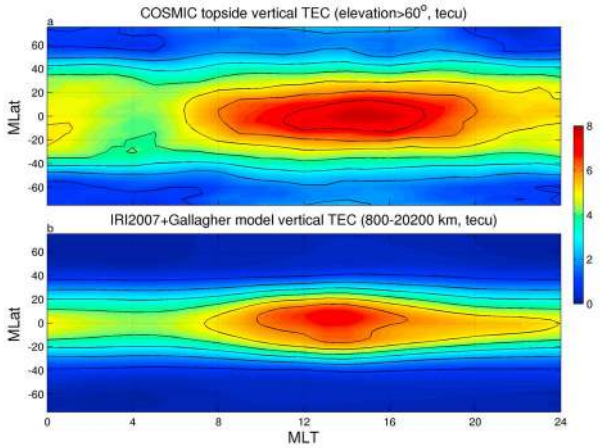

Figure 15. Vertical TEC versus magnetic local time (MLT) and magnetic latitude for (a) COSMIC observations and (b) model results by IRI2007 plus Gallagher plasmasphere between ~800 km and GPS satellite altitude (~20200 km) during 2008 northern spring.

Table 1. Satellite Parameters (Inclination, Orbit Altitude, GPS Receiver Type, Operation Years, POD Antenna Normal) and the Corresponding Error Amplitude (Multipath RMSE for C/A Code, Average Leveling Error, Average DCB RMSE) for the Selected LEO Missions[a]

Mission	Inclination (deg)/Altitude (km)/Mass (kg)	GPS Receiver Type	Operation Years	POD Antenna Normal	Multipath RMSE (C/A, m)	Leveling Error Mean (tecu)	DCB RMSE Mean (tecu)
COSMIC FM4	72/700–800/70	Blackjack	2006-	75° off the zenith	0.30	0.12	0.69
CHAMP	87.3/460–330/522	Blackjack	2000–2009	zenith	0.20	0.19	0.11
GRACE-A	89/~495/432	Blackjack	2002-	zenith	0.42	0.31	0.14
SAC-C	98.2/~710/467	Blackjack	2000-	zenith	0.42	0.60	0.87
TerraSAR-X	97.44/~514/1230	IGOR	2007-	zenith	0.29	0.15	0.09
Metop-A	98.7/~820/4093	GRAS	2006-	zenith	0.15	0.09	0.16

[a]Note that every COSMIC satellite has two POD antennas and only the results of FM 4 antenna 1 are given here.

bending in the ionosphere and the tracking uncertainties of the phase and pseudorange. But the TEC uncertainties resulted from these two factors can be neglectable in comparison with the main error sources listed above. In Figures 1–13 we plot the error distributions of different sources taking example of COSMIC and CHAMP. By our investigation, the TEC errors depend very much on the satellite mission because of the difference in the satellite size, inclination, altitude, thermal control, multipath environment, receiver and antenna type, SNR and etc. In CDAAC, we are currently processing most RO satellite missions if the data are publicly available. Almost all these satellites have one or more POD antennas, which can be used to derive the slant TEC. In Table 1 we list some of these LEO missions, the corresponding satellite parameters and error amplitude including multipath RMSE for C/A code, average leveling error, and average DCB RMSE during a certain time. For COSMIC, only the results of FM 4 antenna 1 are given here since no significant variations of these errors between FMs and two POD antennas have been found. Usually the multipath has a relationship with the satellite size, antenna design and satellite surface configuration [*Montenbruck and Kroes*, 2003]. Although COSMIC is the smallest one during these missions, it has a relatively larger multipath RMSE. This is probably due to its movable solar array panel, which makes the multipath pattern more complicated as illustrated in Figure 3. In the contrary, TerraSAR-X and Metop-A have smaller multipath error RMSE because of difference in the antenna and receiver design, although two satellites is much larger than other missions. As illustrated from the average value of leveling error and DCB RMSE, SAC-C observation is more noise than other missions. COSMIC has a relatively higher DCB RMSE, which might be due to the significant receiver temperature variations because of the lack of the outside protection. These statistical results can be used as a reference when designing the satellite from the point of view of slant TEC. So the accuracy of the slant TEC depends on the mission itself. The RMSE of the colocated slant TEC difference during initial COSMIC stage is ~1.36 tecu as illustrated in Figure 13. Taking account of all these factors, the accuracy of LEO slant TEC can be thought lying between 1 and 3 tecu. This accuracy is adequate in ionosphere study because LEO slant TEC can be as high as hundreds of tecu when passing through the ionosphere in a long distance. More attention should be paid when using high elevation observations to investigate the topside ionosphere and plasmasphere because the TEC amplitude might be comparable with its accuracy. However, statistical results will not be affected as illustrated in Figure 15 and in the work by *Pedatella and Larson* [2010].

[19] LEO based slant TEC, especially the occultation observations in some missions like CHAMP, GRACE-A, and COSMIC, is a good data source of ionosphere data assimilation study because of better global coverage and higher vertical resolution. Figure 16 shows the GPS radio link trajectories over 300 km altitude in ionosphere from COSMIC, CHAMP, and GRACE-A satellites during one

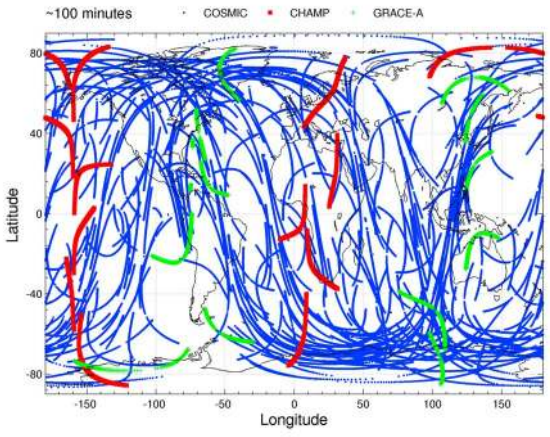

Figure 16. GPS radio link trajectories over 300 km altitude in ionosphere of COSMIC (dot), CHAMP (square), and GRACE-A (cross) satellites during one orbit period (~100 min) of 2008.027. Note that COSMIC observations are from the POD antennas, while CHAMP and GRACE-A are from the occultation antennas.

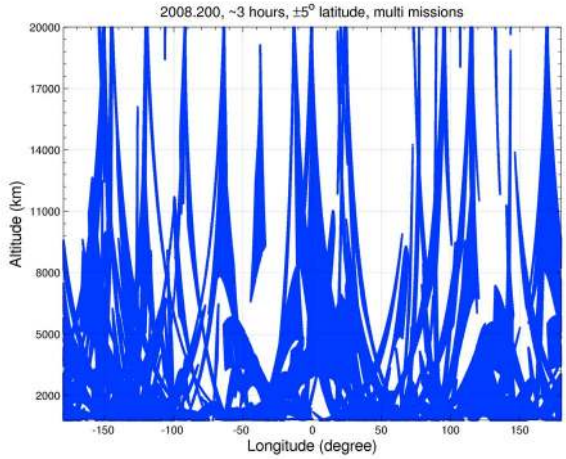

Figure 17. Longitude and altitude (800–20000 km range) variations of the GPS radio link trajectories during 3 h of 2008.200 between ±5° latitude from observations of the COSMIC, CHAMP, GRACE-A, SAC-C, TerraSAR-X, and Metop-A satellites POD antennas.

orbit period (~100 min) of 2008.027. Good global coverage in ionosphere can be found. As described in the introduction section, LEO based observations especially COSMIC observations have shown great potential in ionospheric nowcast, ionospheric drivers estimation, and short-term forecast [*Bust et al.*, 2007; *Komjathy et al.*, 2010; *Pi et al.*, 2009; *Scherliess et al.*, 2009; *Yue et al.*, 2011]. One point we want to emphasize here is that the large numbers of POD observations make imaging three dimensional plasmasphere possible for the first time. Recently, *Spencer and Mitchell* [2011] tried to image the electron density distribution between 800 and 20200 km by using COSMIC observations. Their reconstructed plasmasphere shows obvious response to the interplanetary drivers. Almost most satellites launched recently are equipped with at least one POD antenna for position purpose. To illustrate the data availability in the topside ionosphere and plasmasphere, we plot the GPS radio link trajectories of 3 h during 2008.200 between –5° and +5° latitude range from POD antennas of COSMIC, CHAMP, GRACE-A, SAC-C, TerraSAR-X, and Metop-A satellites in Figure 17. COSMIC and Metop-A data is in 1-Hz sampling while other missions is 10-Hz. We can see these 11 satellites have a very good coverage in the topside ionosphere and plasmasphere in 10° latitude range during 3 h. Taking account of the relatively larger spatial and time scales of the topside ionosphere and plasmasphere, this data availability should be sufficient enough to image the topside ionosphere and plasmasphere.

[20] Furthermore, the elevation of the GPS ray from some missions like COSMIC, CHAMP, and GRACE can be negative by specific design and the tangent point altitude of the GPS rays vary from the LEO altitude to the bottom of the ionosphere, which is recognized as an integer occultation event. An EDP along these tangent points during an occultation event can be retrieved under some assumptions using TEC data by the Abel inversion [*Schreiner et al.*, 1999; *Yue et al.*, 2010]. Some useful ionospheric characteristics including peak density (NmF2) and height (hmF2) are then derived from these EDPs. The Abel inversion has degraded performance in low altitude and latitude region and systematic error distribution [*Yue et al.*, 2010, 2011]. In addition, the observed signal-to-noise intensity fluctuations of the GPS signal can be used to reconstruct the ionospheric S4 index, which is usually selected to monitor the ionospheric scintillation and irregularities [*Sokolovskiy et al.*, 2002]. It should be emphasized that the degraded SNR resulted from the scintillation will effect the accuracy of the determined TEC data. To eliminate the effects of ionosphere on the lower atmosphere retrieval, most occultation receivers like Blackjack onboard CHAMP, GRACE, SAC-C and COSMIC are designed to start sampling at higher altitude (~130–150 km) with high resolution. These high rate data is demonstrated to be useful on monitoring the ionospheric sporadic E (Es) and metal ion layers. All these direct measured or indirect retrieved ionospheric parameters have shown significant value in the past decade on the monitoring and scientific research of ionospheric weather, which is an important part in space weather [*Coster and Komjathy*, 2008; *Hajj et al.*, 2000; *Jakowski et al.*, 2007; *Komjathy et al.*, 2010; *Pedatella et al.*, 2009].

5. Conclusion

[21] In this study, the calculation method of the LEO based GPS slant TEC in CDAAC is generally described. The main error sources, including the multipath calibration, the leveling of the phase TEC to the pseudorange TEC, and the DCB estimation, are quantitatively analyzed for different satellite missions. It is confirmed that the multipath is stable for the same satellite platform and depends on the satellite size, surface, solar panel location, and antenna design. The DCB estimation method based on the spherical symmetry ionosphere assumption agrees well with the quantitative analysis of data from multiple LEO missions. It is suggested that the LEO TEC accuracy might be enhanced if the receiver temperature effect on DCB estimation is considered. The calculated TEC is validated through comparison with the original pseudorange TEC, empirical model, and statistically analyzing the TEC difference between colocated clustered observations of COSMIC during the initial stage. Quantitatively, the accuracy of the LEO slant TEC can be thought lying in 1–3 tecu, depending on the mission. These results are useful for the data users especially when doing data assimilation jobs.

[22] **Acknowledgments.** This paper is based on research supported by the U.S. Air Force with funds awarded via the National Science Foundation under Cooperative Agreement AGS-0918398/CSA AGS-0961147. We thank GFZ-Potsdam for access to the CHAMP, GRACE-A, and TerraSAR-X data; JPL/CONAE for the release of

SAC-C data; and EUMETSAT for providing Metop-A GRAS data. The CHAMP GPS receiver CPU temperature was kindly provided by Jens Wickert and Wolfgang Koehler from GFZ. Part of the paper was based on research done by Stig Syndergaard when he was working at CDAAC/UCAR.

References

Anthes, R. A. (2011), Exploring Earth's atmosphere with radio occultation: Contributions to weather, climate and space weather, *Atmos. Meas. Tech. Discuss.*, *4*, 135–212, doi:10.5194/amtd-4-135-2011.

Bilitza, D. (2009), Evaluation of the IRI-2007 model options for the topside electron density, *Adv. Space Res.*, *44*, 701–706, doi:10.1016/j.asr.2009.04.036.

Blewitt, G. (1990), An automatic editing algorithm for GPS data, *Geophys. Res. Lett.*, *17*, 199–202, doi:10.1029/GL017i003p00199.

Bust, G. S., G. Crowley, T. W. Garner, T. L. Gaussiran II, R. W. Meggs, C. N. Mitchell, P. S. J. Spencer, P. Yin, and B. Zapfe (2007), Four-dimensional GPS imaging of space weather storms, *Space Weather*, *5*, S02003, doi:10.1029/2006SW000237.

Coster, A., and A. Komjathy (2008), Space weather and the Global Positioning System, *Space Weather*, *6*, S06D04, doi:10.1029/2008SW000400.

Foelsche, U., and G. Kirchengast (2002), A simple "geometric" mapping function for the hydrostatic delay at radio frequencies and assessment of its performance, *Geophys. Res. Lett.*, *29*(10), 1473, doi:10.1029/2001GL013744.

Gallagher, D. L., P. D. Craven, and R. H. Comfort (1988), An empirical model of the Earth's plasmasphere, *Adv. Space Res.*, *8*, 15–24, doi:10.1016/0273-1177(88)90258-X.

Hajj, G. A., L. C. Lee, X. Pi, L. J. Romans, W. S. Schreiner, P. R. Straus, and C. Wang (2000), COSMIC GPS ionospheric sensing and space weather, *Terr. Atmos. Oceanic Sci.*, *11*, 235–272.

Heise, S., N. Jakowski, A. Wehrenpfennig, C. Reigber, and H. Lühr (2002), Sounding of the topside ionosphere/plasmasphere based on GPS measurements from CHAMP: Initial results, *Geophys. Res. Lett.*, *29*(14), 1699, doi:10.1029/2002GL014738.

Hwang, C., T.-P. Tseng, T.-J. Lin, D. Švehla, U. Hugentobler, and B. F. Chao (2010), Quality assessment of FORMOSAT-3/COSMIC and GRACE GPS observables: Analysis of multipath, ionospheric delay and phase residual in orbit determination, *GPS Solut.*, *14*, 121–131, doi:10.1007/s10291-009-0145-0.

Jakowski, N., V. Wilken, and C. Mayer (2007), Space weather monitoring by GPS measurements on board CHAMP, *Space Weather*, *5*, S08006, doi:10.1029/2006SW000271.

Komjathy, A., B. Wilson, X. Pi, V. Akopian, M. Dumett, B. Iijima, O. Verkhoglyadova, and A. J. Mannucci (2010), JPL/USC GAIM: On the impact of using COSMIC and ground-based GPS measurements to estimate ionospheric parameters, *J. Geophys. Res.*, *115*, A02307, doi:10.1029/2009JA014420.

Mannucci, A. J., B. D. Wilson, D. N. Yuan, C. H. Ho, U. J. Lindqwister, and T. F. Runge (1998), A global mapping technique for GPS-derived ionospheric total electron content measurements, *Radio Sci.*, *33*(3), 565–582, doi:10.1029/97RS02707.

Mannucci, A. J., B. T. Tsurutani, B. A. Iijima, A. Komjathy, A. Saito, W. D. Gonzalez, F. L. Guarnieri, J. U. Kozyra, and R. Skoug (2005), Dayside global ionospheric response to the major interplanetary events of October 29–30, 2003 "Halloween Storms," *Geophys. Res. Lett.*, *32*, L12S02, doi:10.1029/2004GL021467.

Montenbruck, O., and R. Kroes (2003), In-flight performance analysis of the CHAMP BlackJack GPS Receiver, *GPS Solut.*, *7*, 74–86, doi:10.1007/s10291-003-0055-5.

Pedatella, N. M., and K. M. Larson (2010), Routine determination of the plasmapause based on COSMIC GPS total electron content observations of the midlatitude trough, *J. Geophys. Res.*, *115*, A09301, doi:10.1029/2010JA015265.

Pedatella, N. M., J. Lei, K. M. Larson, and J. M. Forbes (2009), Observations of the ionospheric response to the 15 December 2006 geomagnetic storm: Long-duration positive storm effect, *J. Geophys. Res.*, *114*, A12313, doi:10.1029/2009JA014568.

Pi, X., A. J. Mannucci, B. A. Irijima, B. D. Wilson, A. Komjathy, T. F. Runge, and V. Akopian (2009), Assimilative modeling of ionospheric disturbances with FORMOSAT-3/COSMIC and ground-based GPS measurements, *Terr. Atmos. Oceanic Sci.*, *20*, 273–285, doi:10.3319/TAO.2008.01.04.01(F3C).

Rideout, W., and A. Coster (2006), Automated GPS processing for global total electron content data, *GPS Solut.*, *10*, 219–228, doi:10.1007/s10291-006-0029-5.

Sardón, E., A. Rius, and N. Zarraoa (1994), Estimation of the transmitter and receiver differential biases and the ionospheric total electron content from Global Positioning System observations, *Radio Sci.*, *29*(3), 577–586, doi:10.1029/94RS00449.

Schaer, S. (1999), Mapping and predicting the Earth's ionosphere using the Global Positioning System, Ph.D. dissertation, Astron. Inst., Univ. of Bern, Bern.

Scherliess, L., D. C. Thompson, and R. W. Schunk (2009), Ionospheric dynamics and drivers obtained from a physics-based data assimilation model, *Radio Sci.*, *44*, RS0A32, doi:10.1029/2008RS004068.

Schreiner, W. S., S. V. Sokolovskiy, C. Rocken, and D. C. Hunt (1999), Analysis and validation of GPS/MET radio occultation data in the ionosphere, *Radio Sci.*, *34*(4), 949–966, doi:10.1029/1999RS900034.

Schreiner, W., C. Rocken, S. Sokolovskiy, S. Syndergaard, and D. Hunt (2007), Estimates of the precision of GPS radio occultations from the COSMIC/FORMOSAT-3 mission, *Geophys. Res. Lett.*, *34*, L04808, doi:10.1029/2006GL027557.

Sokolovskiy, S., W. Schreiner, C. Rocken, and D. Hunt (2002), Detection of high-altitude ionospheric irregularities with GPS/MET, *Geophys. Res. Lett.*, *29*(3), 1033, doi:10.1029/2001GL013398.

Spencer, P. S. J., and C. N. Mitchell (2011), Imaging of 3-D plasmaspheric electron density using GPS to LEO satellite differential phase observations, *Radio Sci.*, *46*, RS0D04, doi:10.1029/2010RS004565.

Yue, X., W. S. Schreiner, J. Lei, S. V. Sokolovskiy, C. Rocken, D. C. Hunt, and Y.-H. Kuo (2010), Error analysis of Abel retrieved electron density profiles from radio occultation measurements, *Ann. Geophys.*, *28*, 217–222, doi:10.5194/angeo-28-217-2010.

Yue, X., W. S. Schreiner, Y.-C. Lin, C. Rocken, Y.-H. Kuo, and B. Zhao (2011), Data assimilation retrieval of electron density profiles from radio occultation measurements, *J. Geophys. Res.*, *116*, A03317, doi:10.1029/2010JA015980.

D. C. Hunt, Y.-H. Kuo, C. Rocken, W. S. Schreiner, and X. Yue, COSMIC Program Office, University Corporation for Atmospheric Research, Boulder, CO 80307, USA. (xinanyue@ucar.edu)